



HAL
open science

A translationally optimized AAV-UGT1A1 vector drives safe and long-lasting correction of Crigler-Najjar syndrome

Giuseppe Ronzitti, Giulia Bortolussi, Remco van Dijk, Fanny Collaud, Severine Charles, Christian Leborgne, Patrice Vidal, Samia Martin, Bernard Gjata, Marcelo Simon Sola, et al.

► To cite this version:

Giuseppe Ronzitti, Giulia Bortolussi, Remco van Dijk, Fanny Collaud, Severine Charles, et al.. A translationally optimized AAV-UGT1A1 vector drives safe and long-lasting correction of Crigler-Najjar syndrome. *Molecular Therapy - Methods and Clinical Development*, 2016, 3, 10.1038/mtm.2016.49 . hal-01474146

HAL Id: hal-01474146

<https://hal.sorbonne-universite.fr/hal-01474146>

Submitted on 22 Feb 2017

HAL is a multi-disciplinary open access archive for the deposit and dissemination of scientific research documents, whether they are published or not. The documents may come from teaching and research institutions in France or abroad, or from public or private research centers.

L'archive ouverte pluridisciplinaire **HAL**, est destinée au dépôt et à la diffusion de documents scientifiques de niveau recherche, publiés ou non, émanant des établissements d'enseignement et de recherche français ou étrangers, des laboratoires publics ou privés.



Distributed under a Creative Commons Attribution - NonCommercial - NoDerivatives 4.0 International License

ARTICLE

A translationally optimized AAV-UGT1A1 vector drives safe and long-lasting correction of Crigler-Najjar syndrome

Giuseppe Ronzitti¹, Giulia Bortolussi², Remco van Dijk³, Fanny Collaud¹, Severine Charles¹, Christian Leborgne¹, Patrice Vidal^{1,4}, Samia Martin¹, Bernard Gjata¹, Marcelo Simon Sola¹, Laetitia van Wittenberghe¹, Alban Vignaud¹, Philippe Veron¹, Piter J Bosma³, Andres F Muro² and Federico Mingozzi^{1,4,5}

Crigler-Najjar syndrome is a severe metabolic disease of the liver due to a reduced activity of the UDP Glucuronosyltransferase 1A1 (UGT1A1) enzyme. In an effort to translate to the clinic an adeno-associated virus vector mediated liver gene transfer approach to treat Crigler-Najjar syndrome, we developed and optimized a vector expressing the UGT1A1 transgene. For this purpose, we designed and tested *in vitro* and *in vivo* multiple codon-optimized UGT1A1 transgene cDNAs. We also optimized noncoding sequences in the transgene expression cassette. Our results indicate that transgene codon-optimization is a strategy that can improve efficacy of gene transfer but needs to be carefully tested *in vitro* and *in vivo*. Additionally, while inclusion of introns can enhance gene expression, optimization of these introns, and in particular removal of cryptic ATGs and splice sites, is an important maneuver to enhance safety and efficacy of gene transfer. Finally, using a translationally optimized adeno-associated virus vector expressing the UGT1A1 transgene, we demonstrated rescue of the phenotype of Crigler-Najjar syndrome in two animal models of the disease, Gunn rats and *Ugt1a1*^{-/-} mice. We also showed long-term (>1 year) correction of the disease in Gunn rats. These results support further translation of the approach to humans.

Molecular Therapy — Methods & Clinical Development (2016) **3**, 16049; doi:10.1038/mtm.2016.49; published online 20 July 2016

INTRODUCTION

Crigler-Najjar (CN) syndrome¹ is an ultra-rare (<1 in 1,000,000 individuals at birth^{2,3}) autosomal recessive disease caused by the deficiency of liver-specific UDP Glucuronosyltransferase 1A1 (UGT1A1) enzyme, resulting in the toxic, life-threatening accumulation of unconjugated bilirubin (UCB) in all body tissues, and especially in the brain.^{4,5} Depending on the underlying mutation in the UGT1A1 gene, the severity of CN syndrome can vary from mild to severe.^{6,7} If not promptly treated, the severe form of CN rapidly leads to bilirubin encephalopathy also known as kernicterus, an irreversible and lethal brain damage^{4,8} due to the neurotoxicity of UCB. Presently, severely affected patients are treated by whole-body exposure to phototherapy for up to 10–12 hours/day.^{9,10} This is a cumbersome treatment with important shortcomings like a persistent risk of life threatening spikes of UCB due, for instance, to trauma or sepsis,^{11,12} and a gradual loss of efficacy over time. Orthotopic liver transplantation to restore UGT1A1 activity is the only definitive cure for the severe form of CN syndrome,^{2,10} however this approach presents several risks associated with the procedure^{13,14} and the need for lifelong immunosuppression.¹⁵ In view of all the limitations of the current therapies for CN syndrome, a novel curative treatment based on gene therapy appears to be a therapeutic option for the disease.

Adeno-associated virus (AAV) vector-mediated liver gene transfer has shown promising results in preclinical animal models and, more recently, in humans.^{16–18} AAV vectors are derived and essentially identical to their wild-type counterpart, a small, nonenveloped parvovirus that is nonpathogenic and naturally replication deficient.¹⁹ AAV vectors have become one of the gene therapy vectors of choice for all *in vivo* applications due to their excellent safety profile, poor proinflammatory profile, the fact that they do not efficiently integrate into the host genome, and importantly, the fact that they can drive multiyear expression of a donated transgene in humans.^{17,20} Proof-of-concept of safe, efficacious, long-term correction of a number of diseases targeting the liver with AAV vectors exist in animal models,²¹ including animal models of CN syndrome,^{22–25} and in humans.^{16–18,20} Additionally, several gene therapy trials for inherited liver metabolic disorders have been proposed²⁶ and will likely reach the clinic in the near future.

In addition to the advances in AAV gene transfer to the liver, CN syndrome is an ideal disease model for AAV vector-mediated liver gene transfer for a number of reasons, including (i) the liver of affected individuals is mostly structurally normal²⁷; (ii) the therapeutic window is wide, with levels of UGT1A1 enzyme activity as low as 5%, sufficient to convert the disease from severe to mild^{24,28,29}; (iii) a threshold for clinical benefit is well defined: serum bilirubin

The first four authors contributed equally to this work.

The last three authors shared senior authorship.

¹Genethon, Evry, France; ²International Centre for Genetic Engineering and Biotechnology, Trieste, Italy; ³Tytgat Institute for Liver and Intestinal Research, Academic Medical Center, Amsterdam, the Netherlands; ⁴Universite' Pierre et Marie Curie – Paris 6, Paris, France; ⁵INSERM U951, Evry, France. Correspondence: F Mingozzi (fmingozzi@genethon.fr)

Received 22 May 2016; accepted 3 June 2016

levels below 20 mg/dl in most patients will result in significantly lower risks of brain damage¹⁰; (iv) assessment of therapeutic efficacy is straightforward with clinically well-established assays (e.g., measurement of serum total bilirubin (TB) levels); (v) relevant animal models are available, such as the Gunn rat³⁰ and the *Ugt1a1*^{-/-} mouse²⁴; and (vi) failure to establish correction of the disease with gene transfer for UGT1A1 would not prevent conventional phototherapy from being efficacious or orthotopic liver transplantation from being performed.

Here we developed a novel AAV vector encoding for the UGT1A1 transgene and we optimized the expression cassette for safe and long-term expression in liver. Our results indicate that codon optimization of the transgene, together with intron optimization, results in higher levels of transgene expression and are able to correct the pathological accumulation of UCB in both mice and rats affected by CN syndrome. Moreover, our data indicate that one important determinant of long-term stability of gene transfer in liver is the level of hepatocyte proliferation. Results shown here support the translation of this novel *in vivo* therapeutic approach to humans.

RESULTS

Codon-optimization of the UGT1A1 cDNA leads to higher protein levels in a human hepatocyte cell line

Codon-optimization of the cDNA encoding for a therapeutic transgene has been used to enhance the therapeutic efficacy of AAV vectors.³¹ Here we applied two codon optimization algorithms to the human UGT1A1 cDNA in order to achieve higher expression of the transgene. The two optimized sequences were significantly different from the wild-type cDNA encoding for the UGT1A1 transgene (Table 1), with the version 1 (v1) of the cDNA showing a codon adaptation index (CAI)³² of 0.76, identical to the CAI of the wild-type UGT1A1 sequence (wt). Conversely, the CAI of the version 2 (v2) of the cDNA had an enhanced CAI of 0.96, predictive of higher translational efficiency³² (Figure 1a). Additionally, v1 had similar GC content to the wt cDNA (55.30% and 50.49%, respectively), while GC content in the v2 was higher (60.59%) (Figure 1b), further confirming a higher level of sequence optimization for the v2 sequence.

Next, we determined mRNA and protein expression levels of the wt and codon-optimized UGT1A1 transgenes *in vitro*. Identical expression cassettes were generated based on the liver-specific alpha 1 antitrypsin promoter and apolipoprotein E enhancer (hAAT) promoter, and transfected into a Huh-7 human hepatoma cell line. Levels of mRNA and protein were measured 48 hours after transfection. Slightly higher levels of UGT1A1 mRNA were measured in triplicate testing (Figure 1c), while significantly higher levels of UGT1A1 protein were detectable by western blot in cell lysates following

transfection of the v1 and v2 constructs (Figure 1d, analysis of variance $P = 0.035$ and 0.036 , respectively).

Next, we evaluated whether the UGT1A1 protein was correctly localized to the endoplasmic reticulum, even when overexpressed. Huh-7 cells were transfected in duplicate with the wt, v1, or v2 constructs and the colocalization of the UGT1A1 protein with the 78 kDa glucose related protein (GRP-78) marker was evaluated on an ImageStreamer X system. Representative output of the assay is shown in Figure 1 e,f. In all experiments, staining for UGT1A1 colocalized to the same extent with that for GRP-78 (Figure 1g), indicating that the overexpression of the transgene deriving from codon-optimization did not influence intracellular localization of UGT1A1.

Removal of cryptic ATGs from introns in expression cassette results in higher transgene expression levels

Cryptic translation start codons have been described as potential triggers of transgene immunogenicity.³³ While codon-optimization resulted in removal of alternative open reading frames from the UGT1A1 cDNA (not shown), we focused our attention on the synthetic intron present in the transgene expression cassette. Open reading frames analysis of the sequence of the human hemoglobin subunit beta (HBB2) synthetic intron³⁴ revealed the presence of three ATGs in position 128, 308, and 363, between the splicing donor and splicing acceptor of the intron at position 23 and 392, respectively (Figure 2a).

After elimination of all ATGs, the optimized HBB2 intron and its unmodified counterpart were cloned in a luciferase expressing cassette under the control of the liver-specific hAAT promoter (see Materials and Methods). As controls, luciferase expressing plasmids carrying the SV40 intron (naturally devoid of cryptic ATGs) and the intron 1 of coagulation factor IX³⁵ (untouched or optimized, Supplementary Figure S1) were also generated. Triplicated transient transfection experiments were performed in which the luciferase expression levels were measured and normalized to the SV40 intron construct. Interestingly, optimization of both the HBB2 and the coagulation factor introns led to significantly higher luciferase expression levels in Huh-7 cells (*t*-test, $P = 0.002$ and 0.005 , respectively) (Figure 2b), indicating that cryptic translation start sites present in synthetic introns can negatively influence transgene expression levels.

To identify the mechanism by which the intron optimization influenced transgene expression levels, a primer elongation assay was performed using a reverse oligo localized at the 5' of the luciferase transgene sequence. This oligo was annealed and elongated by reverse transcriptase, using messenger RNA as a template. The schematic representation of the assay is shown in Supplementary Figure S2. Primer elongation analysis of the mRNA isolated from cells transfected with the SV40 and HBB2 constructs revealed the presence of a prominent ~200 bp band corresponding to the predicted fully-processed mRNA, together with two other higher molecular weight (~400 bp) bands corresponding to alternative splicing forms of the mRNA (Figure 2c). These alternatively spliced mRNA forms were not detectable in the optimized HBB2 intron, possibly due to the destabilization of these transcripts. Interestingly, in another set of experiments, we tested luciferase expression levels deriving from constructs carrying HBB2 introns devoid of any splice acceptor sites (splicing incompetent), either carrying or not cryptic ATGs (see Supplementary Figure S3). In these experiments, splicing deficient constructs showed lower levels of luciferase expression compared with the splicing competent construct, and the removal of the cryptic ATGs in the splicing deficient construct resulted in enhanced luciferase expression levels (Figure 2d).

Table 1 Characteristics of wild-type and codon optimized UGT1A1 cDNA sequences

Sequence	Similarity (% versus wt)	CAI ^a (average)	GC content ^c (%)
wt	100	0.76	50.5
v1	77.5	0.76	55.3
v2	78.3	0.96	60.6

^aCodon adaptation index (CAI) and GC content of the three sequences have been calculated using an online codon analysis tool (http://www.genscript.com/cgi-bin/tools/rare_codon_analysis).

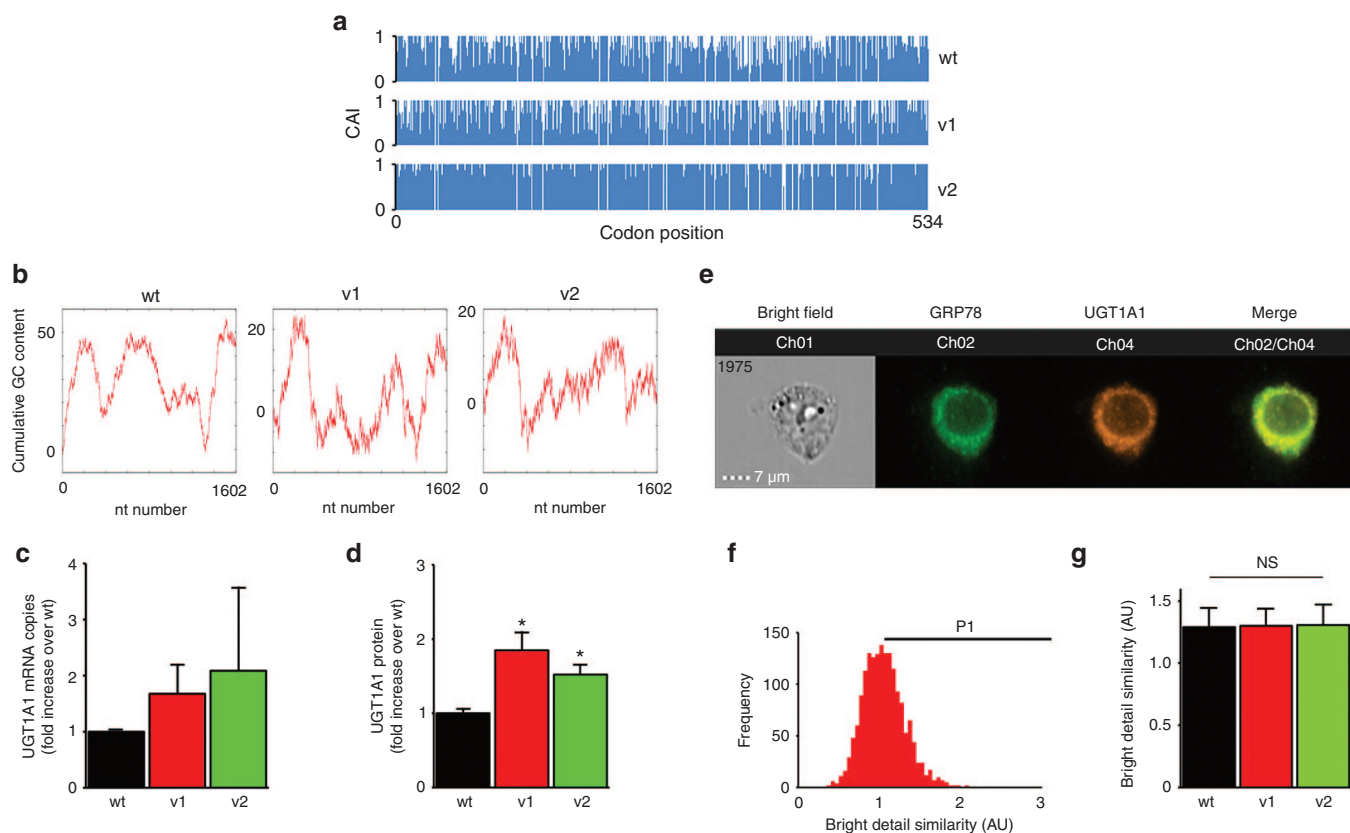


Figure 1 Codon optimization results in higher levels of UGT1A1 transgene expression. Human UGT1A1 wild-type (wtUGT1A1) sequence has been codon optimized following two commercial algorithms (respectively v1UGT1A1 and v2UGT1A1) as described under Materials and Methods. **(a)** Graph showing the codon adaptation index (CAI) for each codon of the wild-type (wt), codon optimized version 1 (v1), and codon optimized version 2 (v2) UGT1A1 cDNA. The CAI = 1 indicates that the frequency of the codons used is the same of that of the most expressed genes in humans. **(b)** Cumulative GC nucleotides content of wt, v1, and v2 UGT1A1 cDNAs. **(c,d)** The wt, v1, and v2 UGT1A1 transgenes were expressed under the control of the hAAT promoter in Huh-7 cells. 48 hours post-transfection mRNA **(c)** and protein **(d)** levels were analyzed. Data are expressed as mean \pm SEM of triplicate experiments. Statistical analyses in panel **c** and **d** have been performed by analysis of variance (ANOVA) ($*P < 0.05$). UGT1A1 mRNA levels were normalized to the expression levels of albumin and then normalized for the levels measured in cells transfected with the wtUGT1A1 plasmid. UGT1A1 protein levels were normalized on the level of calnexin and then to the levels observed in cells transfected with the wtUGT1A1 plasmid. **(e-g)** Huh-7 cells were transfected with wtUGT1A1, v1UGT1A1 or v2UGT1A1. After 48 hours of transfection, cells were trypsinized and stained for 78 kDa glucose-regulated proteins (GRP78) and UGT1A1, as described in Materials and Methods. Cells were acquired at 60 \times using ImageStreamX Mark II Imaging Flow Cytometer. **(e)** Example of imaging of UGT1A1 transfected cells. Ch01, bright field; Ch02, in green, channel corresponding to the GRP78 staining; Ch04, in orange, channel corresponding to UGT1A1 staining. Channel Ch02/Ch04 shows the fluorescence overlay and in yellow, the regions of the cell where the two staining colocalizes. **(f)** The graph shows the frequency of the Bright Detail similarity for GRP78 and UGT1A1 used for colocalization analysis. **(g)** Statistical analysis of the bright detail similarity obtained in cells transfected with wtUGT1A1, v1UGT1A1 or v2UGT1A1. In the graph are shown the median \pm SD of the bright detail similarity of P1 population. Statistical analysis has been performed by ANOVA ($*P < 0.05$). UGT1A1, UDP Glucuronosyltransferase 1A1; SD, standard deviation; SEM, standard error of mean; hAAT, human alpha 1-antitrypsin.

Together these results indicate that the presence of cryptic ATGs in introns can negatively influence transgene expression levels. This negative effect correlates, at least for the HBB2 synthetic intron, with the presence of unprocessed and partially processed forms of mRNA. This leads to the formation of mRNAs containing cryptic ATGs that are inefficiently transcribed and possibly leading to the production of aberrant proteins.

Next, we produced AAV8 vectors carrying the UGT1A1 transgene under the control of the hAAT promoter and carrying either the HBB2 or the optimized, ATG-free HBB2 intron. AAV8 vectors were injected intraperitoneally (i.p.) at escalating doses to *Ugt1a1*^{-/-} mice at postnatal day 11 (P11). *Ugt1a1*^{-/-} mice present a phenotype that closely resembles the human condition, therefore unless treated they need to be exposed to phototherapy to survive.^{24,36} Phototherapy was discontinued two days after gene transfer and the animals were housed in normal light conditions. One-month post injection plasma bilirubin levels were determined. We reported a partial correction of serum TB levels (\sim 2.0 mg/dl or 34 μ mol/l) at

the lowest vector dose (1.5E9 vector genomes (vg)/mouse, corresponding to 3.0E11 vg/kg). This level of TB is considered well below the limit of toxicity.^{25,36} We observed a dose-dependent effect on TB levels, reaching the levels of wild type littermates²⁴ at the highest dose, corresponding to 1.6E12 vg/kg (8.0E9 vg/mouse). In the mid- and high-dose treatment groups, lower levels of TB (although not statistically significant) were measured in animals treated with the construct carrying the optimized HBB2 intron (Figure 2e).

The degree of codon-optimization does not accurately predict UGT1A1 transgene expression levels *in vivo*

Based on codon optimization results (Figure 1) we developed three AAV8 vectors expressing the UGT1A1 transgene under the control of the hAAT promoter, AAV8-hAAT-wtUGT1A1, AAV8-hAAT-v1UGT1A1, and AAV8-hAAT-v2UGT1A1. All constructs carried the optimized HBB2 intron.

Vectors were produced, titered side by side and injected via the tail vein into 6 to 8-weeks old Gunn rats²² ($n = 10$ /group) and TB was

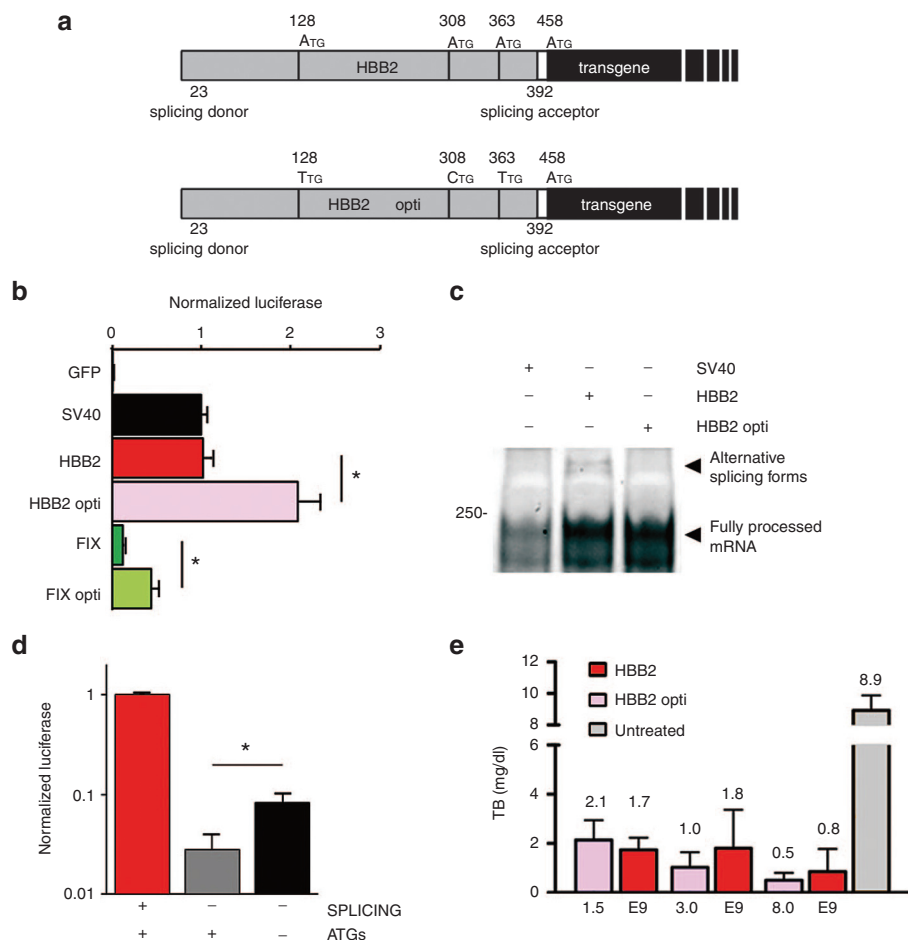


Figure 2 Intron sequence optimization results in higher transgene expression. **(a)** Schematic diagram illustrating the position of ATGs, splicing donor and splicing acceptor in the sequence of the HBB2 intron. The position is calculated from the start of the HBB2 intron (441 bp). The optimized version of the intron (HBB2 opti) does not contain ATGs. **(b)** Huh-7 cells were transfected with plasmids expressing GFP or luciferase fused with introns SV40, HBB2, HBB2 opti, coagulation factor IX (FIX) and FIX opti, described in Materials and Methods, under the transcriptional control of a liver specific promoter. The graph shows the mean \pm SD of luciferase levels measured 48 hours after transfection and normalized to the levels observed with construct carrying the SV40 intron. Data derived from three independent experiments, statistical analysis was performed by nonparametric *t*-test ($*P < 0.05$). **(c)** Primer elongation assay performed on the mRNA obtained from Huh-7 cells transfected with a plasmid expressing firefly luciferase fused with the SV40, the HBB2 intron or its optimized version. The size of the band of a molecular weight standard running in parallel with the sample is indicated on the left. **(d)** Huh-7 cells were transfected with plasmids expressing luciferase under the transcriptional control of a liver specific promoter and fused with the HBB2 intron (in red), the HBB2 sequence mutagenized to remove all the predicted splicing sites (in gray) or the same sequence mutagenized to remove all the predicted splicing sites and all the cryptic ATGs (in black). The graph shows the mean \pm SD of luciferase levels measured in three different samples 48 hours after transfection and normalized on the levels observed in first sample. Data derived from three independent experiments, statistical analysis has been performed by nonparametric *t*-test ($*P < 0.05$). **(e)** Total plasma bilirubin levels (TB) in mutant mice treated with the indicated doses of AAV8 vectors (expressed in vg/mouse) containing the UGT1A1 transgene under the control of the hAAT promoter and carrying either the HBB2 (in red) or the optimized HBB2 intron (in pink). TB levels were measured 1 month postinjection. For each dose/vector $n = 4$. Untreated animals (in gray) were used as negative control ($n = 4$). UGT1A1, UDP Glucuronosyltransferase 1A1; SD, standard deviation; HBB2, human hemoglobin beta (HBB)-derived synthetic intron.

measured over time for about 7 weeks after vector delivery. Gunn rats have a milder phenotype compared with *Ugt1a1*^{-/-} mice, as they do not need phototherapy to survive despite the high serum levels of TB (8.2 ± 1.9 mg/dl or 140 ± 32 μ mol/l, mean \pm SD, in our colony). At a dose of $5E10$ vg/kg, partial correction of TB levels was observed with all 3 constructs tested, however, the v2 construct, the one displaying the highest CAI and GC content (Figure 1a, b, respectively), resulted in the lowest and most transient levels of correction of serum TB (Figure 3a, left), indicating lower potency. At a higher vector dose, $5E11$ vg/kg, full correction of TB levels was observed in all animals treated (Figure 3a, right), comparable to those of wild-type animals (0.2 ± 0.3 mg/dl, or 3.3 ± 4.6 μ mol/l, in our colony). No difference in expression levels was observed in animals treated with the wt or v1 UGT1A1 constructs, regardless of the dose

administered (Figure 3a). No statistical differences in serum TB levels were observed between male and female animals from the same treatment cohorts (two-way analysis of variance, sex per treatment, $P > 0.05$ for all treatments).

Vector genome copy number (VGCN) and mRNA levels were also measured in all treated animals, 50 days after vector administration. While VGCN/cell were similar in animals treated with the three vectors (Figure 3b), animals treated with the v2UGT1A1 vector construct showed slightly lower levels of mRNA in liver compared with wt and v1 UGT1A1 treated animals, particularly at the low vector dose (Figure 3c). Differences in mRNA levels were not statistically significant.

Being the UGT1A1 transgene based on the human sequence, we also measured antitransgene antibodies. As already reported,²²

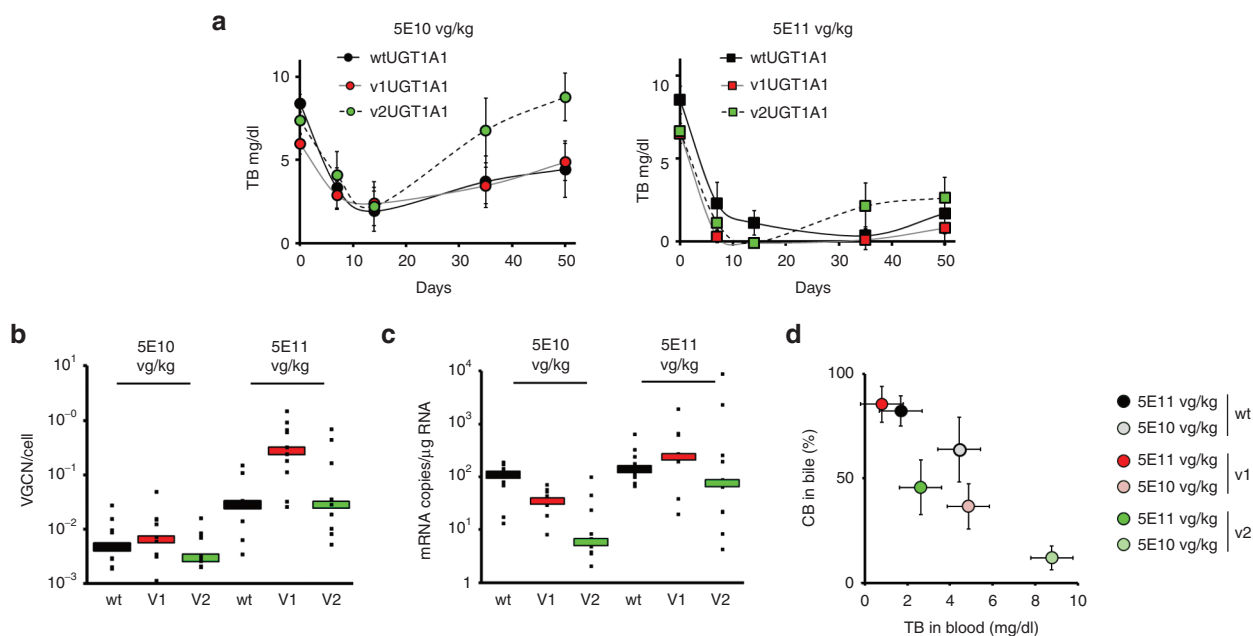


Figure 3 Comparison of the therapeutic efficacy of AAV8 vectors carrying the wt, v1, or v2 UGT1A1 transgenes in Gunn rats. **(a)** Animals ($n = 5$ females and 5 males) were injected with AAV8 vectors expressing the wtUGT1A1 (black), v1UGT1A1 (red), and v2 UGT1A1 (green) transgene at the dose of 5E10 (left) and 5E11 vg/kg (right). Animals were bled weekly and sacrificed two months after the injection of the vectors. Results are shown as mean \pm SD. **(b)** Vector genome copy number (VGCN) per cell measured by qPCR. Values were normalized to the number of copies of titin measured in each sample. In the figure are shown the single values measured (small black dots) and the median value for each treatment (line with the same color code as in **a**). **(c)** UGT1A1 mRNA levels normalized to the levels of rat albumin mRNA. **(d)** Bilirubin conjugates measured by HPLC in the bile of AAV treated Gunn rats. The graph shows the mean \pm SD of the levels of total conjugated bilirubin observed in bile (CB in bile) as a function of the total bilirubin (TB) measured in serum. Darker colors represented the values observed for the high dose whereas lighter colors represented the low dose. Statistical analysis has been performed by ANOVA ($*P < 0.05$). UGT1A1, UDP Glucuronosyltransferase 1A1; ANOVA, one-way analysis of variance; AAV, adeno-associated virus; HPLC, (high performance liquid chromatography); qPCR, quantitative polymerase chain reaction; SD, standard deviation.

several animals were scored positive for anti-UGT1A1 antibodies in all treatment groups, however these antibodies did not affect transgene expression levels or degree of correction of TB (Supplementary Figure S4).

Finally, as a measure of enzyme activity, we collected bile from all treated animals and measured presence of mono- and di-glucuronidated bilirubin (MCB, and DCB, respectively). Untreated Gunn rats have no detectable conjugated bilirubin in bile.²² Levels of conjugated bilirubin in bile correlated with levels of TB in serum ($R^2 = 0.44$; P -value = $2.33E-8$). Content of conjugated bilirubin (expressed as % of MCB and DCB over TB) was the highest in animals treated with the highest dose of wt and v1 UGT1A1 vectors, 5E11 vg/kg, while bile from animals treated with the highest dose of v2 UGT1A1 had CB levels equal to animals treated with a log lower dose of wt and v1 UGT1A1 vectors (Figure 3d). This highlighted significant differences in phenotype correction among experimental groups. The lowest levels of CB in bile and highest levels of TB in serum were found in animals treated with 5E10 vg/kg of v2UGT1A1 vector (Figure 3d).

These results indicate that the outcome of codon-optimization is highly dependent on the transgene, and that testing transgene expression in multiple models *in vitro* and *in vivo* is key to identify the ideal candidate sequence.

Optimized AAV vectors expressing the UGT1A1 transgene correct the disease phenotype in a severe mouse model of CN syndrome. To assess the ability of the newly developed AAV vector construct to correct the phenotype of CN syndrome in a clinically-relevant scenario, *Ugt1a1*^{-/-} mice were treated at P11 with 1.5E9, 3.0E9, or 8.0E9 vg/mouse of the vectors carrying the wt and v1 transgenes. The v2 transgene was not tested because less efficacious in rats. Complete

correction of serum TB was observed in animals treated with the wt and v1 UGT1A1 transgenes (Figure 4a), to levels undistinguishable from the wild-type littermates.²⁴ Conversely, despite phototherapy, untreated *Ugt1a1*^{-/-} animals shown elevated TB levels in serum. One-month postinjection livers were harvested and VGCN/cell was determined. We showed good correlation of VGCN/cell with TB levels, with the exception of the animals treated with the highest dose of vector, in which lower VGCN/cell in liver (not significant) was measured in v1UGT1A1 treated animals (Figure 4b), despite the completely correction of TB in serum (Figure 4a). This result is likely due to the variability of the assay. Likewise, levels of UGT1A1 protein determined by western blot in livers at sacrifice correlated well with serum TB levels and VGCN/cell results (Figure 4c).

Differently from rats, none of the animals treated developed anti-human UGT1A1 antibodies (Supplementary Figure S5), indicating that the observation in rats was likely to be species-specific.

These results indicate that AAV8-hAAT-UGT1A1 vector mediated liver gene transfer with an optimized expression cassette can correct CN syndrome in a model closely mimicking severely affected individuals.

Long-term correction of CN syndrome with an optimized AAV8-UGT1A1 vector

To assess the ability of the optimized AAV8-hAAT-v1UGT1A1 vector to safely and effectively correct CN syndrome long-term, 6–8 week-old Gunn rats were treated with 5E12 vg/kg of vector delivered via the tail vein. In this experiment, five male and five female animals were treated. Animals were followed for ~400 days after vector delivery. As expected vector genome biodistribution showed the highest levels of VGCN/cell in liver (Supplementary Figure S6a).

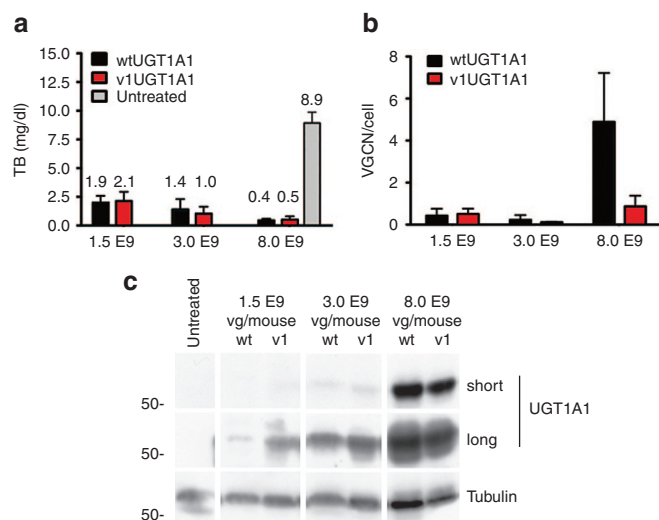


Figure 4 *In vivo* comparison of WT and v1 vectors efficiency in a mouse model of hyperbilirubinemia. **(a)** Total plasma bilirubin levels (TB, mg/dl) in mutant mice treated with escalating doses of optimized AAV8 vectors containing UGT1A1 cDNA. TB levels were measured 1 month post-injection. For each dose/vector, $n \geq 3$. Untreated animals were used as negative control ($n = 4$). **(b)** Viral genome determination (VGCN/cell) performed 1 month post-injection. **(c)** Representative results of the western blot analysis of total liver extracts obtained from UGT1A1 KO mice, untreated or treated with AAV8-UGT1A1 wt or v1 (wt and v1, respectively). In the figure are shown short and long exposure times of the same western blot. Antitubulin was used as loading control. The position of a molecular weight marker running in parallel with the samples is indicated on the left. UGT1A1, UDP Glucuronosyltransferase 1A1; AAV, adeno-associated virus; VGCN, vector genome copy number.

After vector administration, TB levels quickly decreased to undetectable levels and remained undetectable for the duration of the observation period (>1 year) in seven out of 10 animals. This well correlated with VGCN/cell and human UGT1A1 protein levels in liver (Supplementary Figure S6b,c). In three animals, all males, a gradual loss of correction was observed. None of the female rats lost therapeutic efficacy (Figure 5a). At sacrifice, no gross lesions were evident following necropsy performed by a certified pathologist (not shown), however it was noted that male rats had heavier livers compared with females. To further investigate this point, we collected and weighted livers in untreated male and female Gunn rats from birth to 26 weeks of age. This analysis revealed that livers of male rats grew in weight after birth for a longer period of time, and reached larger size than the livers isolated from female rats (Figure 5b). In particular, the liver of male rats appeared still in the growth phase at the time of vector delivery, 6–8 weeks, while in female animals of similar age the liver already reached the final size.

These results indicate that long-term correction of CN syndrome can be achieved in Gunn rats following a single administration of an optimized AAV vector expressing the UGT1A1 transgene. They also correlate the stability of gene transfer with liver growth, suggesting that gene transfer in young children may require later vector readministration.

DISCUSSION

CN syndrome is a rare disease for which the current treatment options are suboptimal and no permanent cure is available except for liver transplantation.^{2,10} Advanced therapies based on allogeneic

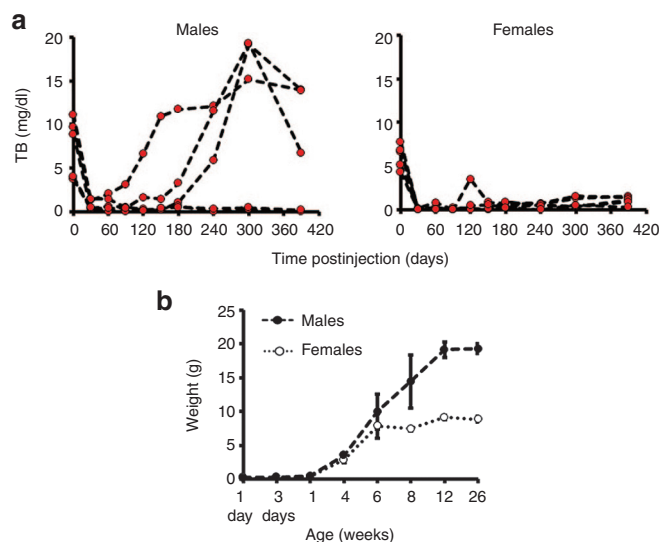


Figure 5 AAV8-UGT1A1 mediates long-term correction of hyperbilirubinemia in a rat model of CN syndrome. 6–8 weeks old male and female Gunn rats ($n = 5$ per group) were intravenously injected with 5E12 vg/kg of AAV8-v1UGT1A1 vector. **(a)** Total bilirubin (TB) levels were measured for 13 months after the injection in serum in male rats (left) and females (right). **(b)** Monitoring of liver growth in Gunn rats. Livers were collected at day 1 (1 d), day 3 (3 d) and between 1 and 26 weeks after birth. In the graph are reported the mean \pm SD of the weight of livers obtained from male and female expressed in grams (g). $n = 3$ per group. UGT1A1, UDP Glucuronosyltransferase 1A1; AAV, adeno-associated virus.

hepatocytes or hepatocyte progenitors have been attempted in CN patients, however achieving only limited and transient benefit,^{28,37,38} likely due to the poor levels of engraftment of transplanted cells. This was also shown in a recent cell transplantation trial.³⁹

Using a translationally optimized AAV-UGT1A1 vector, here we showed that it is possible to obtain long-lasting correction of serum TB in two animal models of the disease, and notably to rescue the lethal phenotype of CN syndrome in *Ugt1a1*^{-/-} mice. Additionally, following a single intravenous infusion of our AAV-UGT1A1 vector, we observed long term (>1 year) correction of TB levels in serum, and the appearance of the MCB and DCB forms of conjugated bilirubin in bile, evidence of restoration of enzyme activity and active bilirubin excretion.²²

We previously published proof-of-concept of correction of CN syndrome with AAV vector mediated gene therapy in Gunn rats²² and *Ugt1a1*^{-/-} mice.^{24,25} Similarly, correction of the CN phenotype was also obtained with helper-dependent adenoviral⁴⁰ and lentiviral⁴¹ vectors. In order to translate these results to humans in an AAV vector-based gene therapy clinical trial, we performed an optimization of the human UGT1A1 expression cassette to achieve complete removal of UCB from serum and enhance the safety and the efficacy of the approach. With this strategy, we were able to obtain full correction of serum TB levels in both mouse and rat models of CN syndrome at vector doses lower than those previously described.^{22,25}

We first codon-optimized the UGT1A1 transgene cDNA, a maneuver that has been broadly employed in the field of gene transfer to enhance transgene expression.^{42,43} In parallel, alternate open reading frames were also removed from the coding sequence of the transgene to avoid unwanted immune responses triggered by aberrant antigens.³³ Results in mice and rats failed to evidence higher levels of TB correction in serum from animals treated with codon-optimized versus wt UGT1A1 transgenes. This is in contrast with

results *in vitro* in human cell lines, which showed superior levels of expression deriving from codon-optimized UGT1A1 cDNA. This result is plausible, as the transgene coding sequences were optimized for expression in human cells. Additionally, it should also be pointed out that the UGT1A1 transgene is a membrane protein, and its activity can only be followed indirectly via bilirubin measures, which makes the *in vivo* readout of expression levels less quantitative when compared with other secreted transgenes.³¹

One unexpected finding was that, in the case of the UGT1A1 transgene, the cDNA with the best CAI (*i.e.*, predicted to be ideally optimized) was also the worse performing *in vivo*. Conversely, the UGT1A1 cDNA version with CAI and GC content closer to the native sequence drove the highest levels of transgene expression *in vitro* in human cell lines, and at least equal levels of expression compared with the wild-type UGT1A1 sequence in *Ugt1a1*^{-/-} mice and Gunn rats. This underscores our poor understanding of some aspect of transgene optimization, for example the role of codon usage in protein folding,⁴⁴ which may play an important role in the function of the membrane protein UGT1A1. It also suggests that when approaching the optimization of a transgene expression cassette, multiple codon-optimization algorithms should be empirically tested.

Next, we examined the role of synthetic intron sequences frequently included in AAV vector expression cassettes to enhance mRNA processing and stability.⁴⁵ Bioinformatics analysis of the HBB2 intron, and of other introns commonly used in gene transfer (Supplementary Table S1), revealed the presence of ATGs that could originate aberrant proteins if incorrectly spliced. Our data indicate that, at least *in vitro*, splicing of synthetic introns does not always occur with 100% efficiency, and that removal of all possible ATGs is essential to enhance transgene expression. This has obviously an impact on the safety of gene transfer, as cryptic ATGs could originate potentially immunogenic proteins.⁴⁶ This is a finding not pertaining exclusively to gene transfer for CN syndrome, thus requiring careful evaluation.

Obtaining therapeutic levels of transgene expression at the lowest vector dose possible is an important goal for AAV vector mediated gene transfer. This is particularly true for what it concerns avoidance of potentially detrimental cytotoxic immune responses directed against transduced hepatocytes.^{17,18,47,48} With the construct we developed, therapeutic levels of transgene expression were measured at doses of AAV8-UGT1A1 vector of 5E11 vg/kg, possibly below the threshold of activation of CD8⁺ T- cells, as suggested by results from the AAV hemophilia B trials,^{16,18,47} although ultimately the efficacy of this approach can only be tested in humans. Importantly, long-term rescue of the hyperbilirubinemic phenotype in Gunn rats, and correction of the disease in *Ugt1a1*^{-/-} mice, the animal model closest to the human condition,²⁴ is highly encouraging. Additional optimization steps could involve the use of novel AAV capsids that target specifically and efficiently human hepatocytes^{49,50} or evolutionary intermediates of ancestor AAVs.⁵¹

Like for other pediatric diseases,²⁶ an ideal scenario for CN syndrome would be to achieve stable, long-lasting correction of the disease in young children. As AAV vectors do not efficiently integrate in the host genome,⁵² it is expected that the transduction of actively replicating liver cells with AAV would lead to at least partial vector dilution over time, with reduction in transgene expression levels. We recently described this by injecting neonate *Ugt1a1*^{-/-} mice with AAV vectors 4 days after birth.²⁵ This led to partial vector dilution over time, resulting in lower levels of transgene expression 17 months after gene transfer, which still remained within the therapeutic range.²⁵

While it is a known fact that proliferation of the neonate liver over time leads to dilution of the effect of gene transfer,⁵³ for diseases like CN syndrome for which the amount of transgene expression needed to rescue the diseased phenotype is relatively low, a single administration of an AAV vector at an appropriate dose may be sufficient to achieve lifelong correction of the disease. This would argue in favor of performing gene transfer in young pediatric subjects. Results presented here in Gunn rats support the idea that gene transfer in a rapidly growing liver leads to a variable therapeutic outcome. How these preclinical results will correlate with the stability of AAV mediated liver gene transfer in children is currently unknown. Based on the growth curve of human liver⁵⁴ it is expected that gene transfer in younger children will be less stable than in adults.¹⁷ Several possible strategies have been proposed to address the issue of loss of efficacy following AAV vector delivery, which include strategies to allow for vector readministration,^{55,56} *in vivo* gene editing,^{57,58} or promoterless integrative AAV vectors.⁵⁹

In summary, our work provides a framework for AAV vector optimization for safe and efficient liver gene transfer for CN syndrome in humans. Our results indicated that empirical testing of codon optimization algorithms for the UGT1A1 transgene, together with careful optimization of the noncoding sequences of the transgene expression cassette, are fundamental steps for the translation of preclinical results to humans. For pediatric diseases like CN syndrome, the age at which gene transfer is performed can have a profound influence on the outcome of gene transfer in terms of transgene persistence.

MATERIALS AND METHODS

Plasmid constructs

The transgene expression cassettes used in this study contained a wild-type (wt) or two codon-optimized cDNA sequences encoding for human UGT1A1 (v1 and v2 respectively). Codon-optimized sequences were obtained using commercially available algorithms and further modified to remove alternate open reading frames. Transgene sequences were cloned in an AAV backbone comprising the wild-type AAV2 ITRs, an enhancer derived from apolipoprotein E gene, and the hAAT promoter. The human hemoglobin beta (HBB)-derived synthetic intron (HBB2)³⁴ and the HBB polyadenylation signal were used in all UGT1A1 expression cassettes. The *in vitro* comparison of luciferase expression levels has been performed with the same expression cassette by replacing the UGT1A1 transgene with the firefly luciferase cDNA. The evaluation of the effect of different introns on the transgene expression levels has been performed by replacing the HBB2 sequence with different intron sequences, namely SV40 intron⁶⁰ and human coagulation factor IX intron 1 (ref. 35). HBB2 and coagulation factor IX intron sequences were also modified by removing the ATGs that originated alternative open reading frames longer than 50 bp. All DNA sequences used in the study were synthesized by GeneCust (Dudelange, Luxembourg).

AAV vectors

AAV vectors used in this study were produced using a slight modification of the adenovirus-free transient transfection methods as described earlier.^{61,62} Briefly, adherent human embryonic kidney cells (HEK293) cells grown in roller bottles were transfected with the three plasmids containing the adenovirus helper proteins, the AAV Rep and Cap genes, and the ITR-flanked transgene expression cassette. After 72 hours of transfection, cells were harvested, lysed by sonication, and treated with benzonase (Merck-Millipore, Darmstadt, Germany). Vectors were then purified using two successive ultracentrifugation rounds in cesium chloride density gradients. Full capsids were collected, the final product was formulated in sterile phosphate buffered saline containing 0.001% of pluronic (Sigma Aldrich, Saint Louis, MO), and stored at -80°C.

Titers of AAV vector stocks were determined using quantitative real-time polymerase chain reaction (qPCR). Viral DNA was extracted using the MagNA Pure 96 DNA and viral NA small volume kit (Roche Diagnostics, Indianapolis, IN) according to manufacturer's instructions. The qPCR was performed in ABI PRISM 7900 HT Sequence Detector using Absolute ROX

mix (Taqman, Thermo Fisher Scientific, Waltham, MA). Specific probe and primers were as follows: forward 5'-GGCGGGCGACTCAGATC-3', reverse 5'-GGGAGGCTGCTGGTGAATATT-3', and probe 5'-AGCCCTGTTTGCTCCTCCGATAACTG-3'.

In vitro experiments

For plasmids transfection, plasmids were transfected using Lipofectamine (Thermo Fisher Scientific) into six-well plates containing 80% confluent Huh-7 cells accordingly to manufacturer's instructions. Green fluorescent protein (GFP) expressing plasmids or untreated cells were included as control in each transfection experiment. After 48 hours of transfection, cells were harvested and frozen at -20 °C until further analysis.

RNA extraction and reverse transcription-quantitative polymerase chain reaction

Total RNA was extracted from cell lysates using Trizol (Thermo Fisher Scientific). DNA contaminants were removed using the Free DNA kit (Thermo Fisher Scientific). Total RNA was reverse-transcribed using random hexamers and the RevertAid H minus first strand cDNA synthesis kit (Thermo Fisher Scientific). Reverse transcription-quantitative polymerase chain reaction was performed using SybrGreen (Thermo Fisher Scientific) with primers specific for the UGT1A1 transgene: forward TTCTGCTGGCCGTGGTGCTGA and reverse AGATCTGAATCACCCACC. The rat albumin expression levels were evaluated using the following primers: forward GTGGAAGAGCCTCAGAAT, reverse TTGGTGAACGAACTAATAGC, and were used to normalize the results across samples. Data were expressed as normalized number of copies of UGT1A1 per µg of RNA.

Microsome extraction and Western blot analysis

Microsome extraction was performed at 4 °C. Frozen cell pellets were resuspended in 300 µl of lysis buffer (20 mmol/l Hepes, 1% Triton X-100) containing protease inhibitor cocktail (Sigma Aldrich) and centrifuged 5 minutes at 100×g. Supernatants were collected and centrifuged 60 minutes at 18,000×g. Pellets were resuspended in 100 µl of 20 mmol/l Hepes and the protein concentration was determined using the BCA Protein Assay kit (Thermo Fisher Scientific), following the manufacturer's instructions.

Microsomal extracts were separated on a 4–12% bis-tris polyacrylamide gel (Thermo Fisher Scientific). The same amount of protein was loaded in each lane. The gel was transferred onto a nitrocellulose membrane and blotted with an anti-UGT1A1 antibody (SantaCruz biotechnology, Santa Cruz, CA) and an anti-actin antibody (Sigma Aldrich), used as loading control. Secondary antibodies and detection system were from Li-Cor Biosciences (Lincoln, NE).

Image Stream X analysis

Huh-7 cells were transfected as indicated above. After 48 hours of transfection, cells were harvested, fixed and permeabilized with the PerFix-nc kit (Beckmann Coulter, Brea, CA). Cells were then stained with a rat anti-human UGT1A1 antibody and an anti-78 kDa glucose related protein (GRP-78) as primary antibody (StressMarq, Cadboro Bay, Canada) and then with anti-rabbit AlexaFluor 488 and an anti-rat AlexaFluor 594 secondary antibodies (Thermo Fisher Scientific). Cells were analyzed at a magnification of 60× on an Image Stream X flow imaging equipment (Merck-Millipore). Image analysis was performed using the IDEAS analysis software v6.1 (Merck-Millipore). Single-color controls were used for the creation of a compensation matrix that was applied to all files to correct for spectral cross-talk. Cells in focus were gated based on the fluorescence levels observed in the two channels considering the nonspecific signal obtained with a nonspecific rat serum. Images with a bright detail similarity score >1.2 were used to compare the endoplasmic reticulum localization of UGT1A1 expressed by the three different codon optimization constructs.

Primer elongation assay

A diagram of the primer elongation assay is shown as Supplementary Figure S2. Total RNA was extracted from Huh-7 cells using Trizol. Primer elongation has been performed as already described.⁶³ Briefly, 5 µg of total RNA were retrotranscribed using the RevertAid H minus first strand cDNA synthesis kit (Thermo Fisher Scientific) and a reverse IR-Dye 700 conjugated oligo (IDT technology, Coralville, IA) GTGATCCACAGCCATGGTG specific for

the firefly luciferase sequence. Samples were then separated on a 6% tris-borate-EDTA-Urea gel (Thermo Fisher Scientific) and the gel was acquired using an Odyssey scanner (Li-Cor Biosciences)

Animal experiments

Ugt1a1^{-/-} mice have been described previously.²⁴ Wild type littermates were used as controls in all experiments. Mice were housed and handled according to institutional guidelines, and experimental procedures approved by International Centre for Genetic Engineering and Biotechnology board. Animals used in this study were at least 99.8% C57BL/6 genetic background, obtained after > 9 backcrosses with wild type C57BL/6 mice. Mice were kept in a temperature-controlled environment with 12/12 hour light–dark cycle. They received a standard chow diet and water *ad libitum*.

The Gunn rat is a natural occurring model of CN syndrome that has no residual UGT1A1 enzyme activity.⁶⁴ Rats were fed *ad libitum* and were housed and handled according to institutional guidelines. All *in vivo* experimental procedures were approved by the French, Dutch, and Italian competent authorities and Ethical Committees (ref. 2013007B) according to the European Directive 2010/63/EU.

Gene transfer procedure and phototherapy treatment

For the AAV gene transfer procedure, mice pups at postnatal day 11 (P11) were i.p. injected with AAV8-UGT1A1 vectors or saline. Newborns were exposed to blue fluorescent light (Philips, Amsterdam, The Netherlands) for 12 hours per day (synchronized with the light period of the light/dark cycle) up to 12 days after birth and then maintained under normal light conditions. Intensity of the blue lamps was monitored monthly with an Olympic Mark II Bili-Meter (Olympic Medical, Port Angeles, WA). Blood samples were collected 1 month postinjection in mutant and untreated mutant littermates by facial vein exsanguination or cardiac puncture.

Rats of 6–8 weeks old, were injected i.v. via the tail vein with AAV8-UGT1A1 vectors or saline. Blood samples were collected by retro-orbital venipuncture every week after AAV injection. To determine UGT1A1 expression, liver tissues were collected 2 months post AAV-injection. For the long term follow-up, blood samples were collected every month after AAV injection. Livers and other organs were collected 13 months post AAV-injection.

Bilirubin measurement

TB determination in mice and rats was performed in plasma as previously described. Plates were read at 560nm on an Enspire plate reader (Perkin Elmer, Waltham, MA). Bilirubin conjugates in bile were analyzed and quantified by high performance liquid chromatography as previously described²² using an Omnisphere column (Varian, Palo Alto, CA) for the separation of bilirubin conjugates.⁶⁵

Virus vector genome copy number analysis

To reduce variability generated by uneven transduction of liver parenchyma by AAV vectors, whole rat livers were homogenized in 20 mmol/l Hepes, 250 mmol/l sucrose. For mouse samples, livers were harvested 1 month postinjection, pulverized in liquid nitrogen and aliquoted for further molecular analysis.

Total DNA was extracted using the MagNA Pure 96 DNA and viral NA small volume kit (Roche Diagnosis, Basel, Switzerland) according to manufacturer's instructions. VGCN measured by qPCR were normalized by the copies of titin gene measured in each sample. qPCR was performed on an ABI PRISM 7900 HT Sequence Detector (Agilent Technologies, Santa Clara, CA) using Absolute ROX mix (Thermo Fisher Scientific) and the following specific primers and probes: UGT1A1 forward 5'-GGCGGGCGACTCAGATC-3', reverse 5'-GGGAGGCTGCTGGTGAATATT-3', probe 5'-AGCCCTGTTTGCTCCTCCGATAACTG-3'; titin forward 5'-AGAGGTAGTATTGAAAACGAGCGG-3', reverse 5'-GCTAGCGCTCCCGCTGCTGAAGCTG-3', and probe 5'-TGCAAGGAAGCTTCTCGTCTCAGTC-3'.

VGCN in mice was quantified by qPCR using specific primers for the hAAV promoter as previously described.²⁵

Western blot analysis

Microsomes extraction was performed at 4°C. The resulting material was resuspended in microsome buffer and the protein concentration was determined by Pierce BCA Protein Assay (Thermo Fisher Scientific), following manufacturer's instructions. Western blot on microsomal extracts was performed as described

above with anti-UGT1 rabbit polyclonal antibody (SantaCruz Biotechnology). Anti-actin (Sigma Aldrich), or anti tubulin antibodies (Developmental Studies Hybridoma Bank, Iowa City, IA) were used as loading controls.

For mouse samples, liver powder was homogenized in lysis buffer containing 150 mmol/l NaCl, 1% nonidet-P40, 0.5% sodium deoxicolate, 0.1% sodium dodecyl sulfate, 50 mmol/l Tris HCl pH8 and protease inhibitors and analyzed by Western blot analysis as described previously.²⁴

Anti-UGT1A1 antibody determination

Maxisorp 96 wells plates (Thermo Fisher Scientific) were coated with UGT1A1 protein in carbonate buffer at 4 °C overnight. A standard curve of rat recombinant IgG (Sigma Aldrich) was coated to the wells in seven twofold dilution starting from 1 µg/ml. After blocking, plasma samples were added to plates and incubated 1 hour at 37 °C. Detection was performed by adding to the wells 3,3',5,5'-tetramethylbenzidine substrate (BD Biosciences, San Diego, CA), and color development was measured at 450 and 570 nm (for background subtraction) on an Enspire plate reader (Perkin Elmer) after blocking the reaction with H₂SO₄.

To detect antibodies against the human UGT1A1 protein in mice, 20 µg of total cell protein extract from HEK293 cells transfected with a plasmid expressing the human UGT1A1 cDNA or from untransfected HEK293 cells were run in 10% Sodium dodecyl sulfate polyacrylamide gel electrophoresis gel, blotted onto a nitrocellulose membrane and blocked with 5% milk in Phosphate buffered saline with Tween 20. Plasma from individual animals was used as primary antibody (1:200).

A positive control plasma from mice immunized with recombinant human UGT1A1 was used (1:2,000). A band corresponding to the UGT1A1 protein is detected if antibodies against UGT1A1 are present in the plasma of the AAV-treated animals.

Statistics

Results are expressed as mean ± SEM or mean ± SD as described in the text. The Prism package version 7 (GraphPad Software, La Jolla, CA) or StatistiXL plugin for windows Excel were used to analyze data and prepare the graphs. Statistical analyses have been performed by t-test and one way or two-way analysis of variance as described in the text. Values of $P < 0.05$ were considered as statistically significant.

CONFLICT OF INTEREST

G.B., P.J.B., F.C., A.M., F.M., and G.R. are inventors in patents describing the AAV technology and gene therapy-based treatments for Crigler-Najjar syndrome. P.J.B. consulted on the topic of CN syndrome. All other authors declare no conflict of interests with the work presented here.

ACKNOWLEDGMENTS

This work was supported by Genethon, by the Association Française contre les Dystrophies Musculaire (AFM), the ZonMW grant to P.J.B., the Najjar fund to P.J.B., the European Research Council ERC-2013-CoG grant 617432 to F.M., the Beneficentia Stiftung to A.F.M., the AXA Research Fund to G.B., the EU Marie Skłodowska-Curie fellowship AMD-658712-3 to G.R.

P.J.B., A.M., and F.M. contributed to the experimental design, supervised experiments and results interpretation, and wrote the manuscript. G.R., G.B., R.v.D., and F.C. contributed to experimental design, performed experiments and analyzed the data, contributed to results interpretation and manuscript preparation. S.C., L.v.W., and A.V. contributed to the in vivo experiments. C.L., P.V., S.M., B.G., M.S.S., and P.V. contributed to the experimental activities.

REFERENCES

- Crigler, JF, Jr, Najjar, VA (1952). Congenital familial nonhemolytic jaundice with kernicterus. *Pediatr* **10**: 169–180.
- van der Veere, CN, Sinaasappel, M, McDonagh, AF, Rosenthal, P, Labrune, P, Odièvre, M et al. (1996). Current therapy for Crigler-Najjar syndrome type 1: report of a world registry. *Hepato* **24**: 311–315.
- Chowdhury, J, Wolkoff, A, Chowdhury, N and Arias, I. Hereditary jaundice and disorders of bilirubin metabolism. In: *The Metabolic and Molecular Bases of Inherited Disease, vol. 2*. McGraw-Hill, New York, 2001. pp. 3063–3101.

- Erlinger, S, Arias, IM and Dhumeaux, D (2014). Inherited disorders of bilirubin transport and conjugation: new insights into molecular mechanisms and consequences. *Gastroenterol* **146**: 1625–1638.
- Bosma, PJ (2003). Inherited disorders of bilirubin metabolism. *J Hepatol* **38**: 107–117.
- Kadacol, A, Ghosh, SS, Sappal, BS, Sharma, G, Chowdhury, JR and Chowdhury, NR (2000). Genetic lesions of bilirubin uridine-diphosphoglucuronate glucuronosyltransferase (UGT1A1) causing Crigler-Najjar and Gilbert syndromes: correlation of genotype to phenotype. *Hum Mutat* **16**: 297–306.
- Skierka, JM, Kotzer, KE, Lagerstedt, SA, O'Kane, DJ and Baudhuin, LM (2013). UGT1A1 genetic analysis as a diagnostic aid for individuals with unconjugated hyperbilirubinemia. *J Pediatr* **162**: 1146–52, 1152.e1.
- Labrune, PH, Myara, A, Francoal, J, Trivin, F and Odièvre, M (1992). Cerebellar symptoms as the presenting manifestations of bilirubin encephalopathy in children with Crigler-Najjar type I disease. *Pediatr* **89**(4 Pt 2): 768–770.
- Ostrow, JD (1971). Photocatabolism of labeled bilirubin in the congenitally jaundiced (Gunn) rat. *J Clin Invest* **50**: 707–718.
- Strauss, KA, Robinson, DL, Vreman, HJ, Puffenberger, EG, Hart, G and Morton, DH (2006). Management of hyperbilirubinemia and prevention of kernicterus in 20 patients with Crigler-Najjar disease. *Eur J Pediatr* **165**: 306–319.
- Sellier, AL, Labrune, P, Kwon, T, Boudjemline, AM, Deschènes, G and Gajdos, V (2012). Successful plasmapheresis for acute and severe unconjugated hyperbilirubinemia in a child with crigler najjar type I syndrome. *JIMD Rep* **2**: 33–36.
- Kaneko, K, Takei, Y, Aoki, T, Ikeda, S, Matsunami, H and Lynch, S (2000). Bilirubin adsorption therapy and subsequent liver transplantation cured severe bilirubin encephalopathy in a long-term survival patient with Crigler-Najjar disease type I. *Intern Med* **39**: 961–965.
- Adam, R, Karam, V, Delvart, V, O'Grady, J, Mirza, D, Klempnauer, J et al.; All contributing centers. www.eltr.org. European Liver and Intestine Transplant Association (ELITA). (2012). Evolution of indications and results of liver transplantation in Europe. A report from the European Liver Transplant Registry (ELTR). *J Hepatol* **57**: 675–688.
- Immordino, G. et al. (2014). Predictability and survival in liver replantation: monocentric experience. *Transplantation proceedings* **46**, 2290–2292.
- Pedersen, M and Seetharam, A (2014). Infections after orthotopic liver transplantation. *J Clin Exp Hepatol* **4**: 347–360.
- Manno, CS, Pierce, GF, Arruda, VR, Glader, B, Ragni, M, Rasko, JJ et al. (2006). Successful transfusion of liver in hemophilia by AAV-Factor IX and limitations imposed by the host immune response. *Nat Med* **12**: 342–347.
- Nathwani, AC, Reiss, UM, Tuddenham, EG, Rosales, C, Chowdhury, P, McIntosh, J et al. (2014). Long-term safety and efficacy of factor IX gene therapy in hemophilia B. *N Engl J Med* **371**: 1994–2004.
- Nathwani, AC, Tuddenham, EG, Rangarajan, S, Rosales, C, McIntosh, J, Linch, DC et al. (2011). Adenovirus-associated virus vector-mediated gene transfer in hemophilia B. *N Engl J Med* **365**: 2357–2365.
- Muzyczka, N and Berns, KI (2001). *Parvoviridae: The Viruses and their Replication*, 4th edn. Lippincott, Williams and Wilkins, Philadelphia.
- Buchlis, G, Podsakoff, GM, Radu, A, Hawk, SM, Flake, AW, Mingozzi, F et al. (2012). Factor IX expression in skeletal muscle of a severe hemophilia B patient 10 years after AAV-mediated gene transfer. *Blood* **119**: 3038–3041.
- Mingozzi, F and High, KA (2011). Therapeutic *in vivo* gene transfer for genetic disease using AAV: progress and challenges. *Nat Rev Genet* **12**: 341–355.
- Seppen, J, Bakker, C, de Jong, B, Kunne, C, van den Oever, K, Vandenberghe, K et al. (2006). Adeno-associated virus vector serotypes mediate sustained correction of bilirubin UDP glucuronosyltransferase deficiency in rats. *Mol Ther* **13**: 1085–1092.
- Pastore, N, Nusco, E, Vanikova, J, Sepe, RM, Vetrini, F, McDonagh, A et al. (2012). Sustained reduction of hyperbilirubinemia in Gunn rats after adeno-associated virus-mediated gene transfer of bilirubin UDP-glucuronosyltransferase isozyme 1A1 to skeletal muscle. *Hum Gene Ther* **23**: 1082–1089.
- Bortolussi, G, Zentilin, L, Baj, G, Giraudi, P, Bellarosa, C, Giacca, M et al. (2012). Rescue of bilirubin-induced neonatal lethality in a mouse model of Crigler-Najjar syndrome type I by AAV9-mediated gene transfer. *FASEB J* **26**: 1052–1063.
- Bortolussi, G, Zentilin, L, Vanikova, J, Bockor, L, Bellarosa, C, Mancarella, A et al. (2014). Life-long correction of hyperbilirubinemia with a neonatal liver-specific AAV-mediated gene transfer in a lethal mouse model of Crigler-Najjar Syndrome. *Hum Gene Ther* **25**: 844–855.
- Junge, N, Mingozzi, F, Ott, M and Baumann, U (2015). Adeno-associated virus vector-based gene therapy for monogenetic metabolic diseases of the liver. *J Pediatr Gastroenterol Nutr* **60**: 433–440.
- Fagioli, S, Daina, E, D'Antiga, L, Colledan, M and Remuzzi, G (2013). Monogenic diseases that can be cured by liver transplantation. *J Hepatol* **59**: 595–612.
- Fox, IJ, Chowdhury, JR, Kaufman, SS, Goertzen, TC, Chowdhury, NR, Warkentin, PI et al. (1998). Treatment of the Crigler-Najjar syndrome type I with hepatocyte transplantation. *N Engl J Med* **338**: 1422–1426.
- Sneitz, N, Bakker, CT, de Knecht, RJ, Halley, DJ, Finel, M and Bosma, PJ (2010). Crigler-Najjar syndrome in The Netherlands: identification of four novel UGT1A1 alleles, genotype-

- phenotype correlation, and functional analysis of 10 missense mutants. *Hum Mutat* **31**: 52–59.
30. Iyanagi, T (1991). Molecular basis of multiple UDP-glucuronosyltransferase isoenzyme deficiencies in the hyperbilirubinemic rat (Gunn rat). *J Biol Chem* **266**: 24048–24052.
 31. Nathwani, AC, Gray, JT, Ng, CY, Zhou, J, Spence, Y, Waddington, SN *et al.* (2006). Self-complementary adeno-associated virus vectors containing a novel liver-specific human factor IX expression cassette enable highly efficient transduction of murine and nonhuman primate liver. *Blood* **107**: 2653–2661.
 32. Sharp, PM and Li, WH (1987). The codon Adaptation Index—a measure of directional synonymous codon usage bias, and its potential applications. *Nucleic Acids Res* **15**: 1281–1295.
 33. Li, C, Goudy, K, Hirsch, M, Asokan, A, Fan, Y, Alexander, J *et al.* (2009). Cellular immune response to cryptic epitopes during therapeutic gene transfer. *Proc Natl Acad Sci USA* **106**: 10770–10774.
 34. Snyder, RO, Spratt, SK, Lagarde, C, Bohl, D, Kaspar, B, Sloan, B *et al.* (1997). Efficient and stable adeno-associated virus-mediated transduction in the skeletal muscle of adult immunocompetent mice. *Hum Gene Ther* **8**: 1891–1900.
 35. Miao, CH, Ohashi, K, Patijn, GA, Meuse, L, Ye, X, Thompson, AR *et al.* (2000). Inclusion of the hepatic locus control region, an intron, and untranslated region increases and stabilizes hepatic factor IX gene expression *in vivo* but not *in vitro*. *Mol Ther* **1**: 522–532.
 36. Bortolussi, G, Baj, G, Vodret, S, Viviani, G, Bittolo, T and Muro, AF (2014). Age-dependent pattern of cerebellar susceptibility to bilirubin neurotoxicity *in vivo* in mice. *Dis Model Mech* **7**: 1057–1068.
 37. Ambrosino, G, Varotto, S, Strom, SC, Guariso, G, Franchin, E, Miotto, D *et al.* (2005). Isolated hepatocyte transplantation for Crigler-Najjar syndrome type 1. *Cell Transplant* **14**: 151–157.
 38. Horslen, SP, McCowan, TC, Goertzen, TC, Warkentin, PI, Cai, HB, Strom, SC *et al.* (2003). Isolated hepatocyte transplantation in an infant with a severe urea cycle disorder. *Pediatr* **111**(6 Pt 1): 1262–1267.
 39. Dobbelaere, D *et al.* (2014). Phase I/II multicenter trial of liver derived mesenchymal stem cells (HepastemR) for the treatment of urea cycle disorder and Crigler Najjar syndrome interim analysis at 6 months post infusion. *J Inherited Metab Dis* **37**: O-027.
 40. Dimmock, D, Brunetti-Pierri, N, Palmer, DJ, Beaudet, AL and Ng, P (2011). Correction of hyperbilirubinemia in Gunn rats using clinically relevant low doses of helper-dependent adenoviral vectors. *Hum Gene Ther* **22**: 483–488.
 41. Schmitt, F, Remy, S, Dariel, A, Flageul, M, Pichard, V, Boni, S *et al.* (2010). Lentiviral vectors that express UGT1A1 in liver and contain miR-142 target sequences normalize hyperbilirubinemia in Gunn rats. *Gastroenterol* **139**: 999–1007, 1007.e1.
 42. Binny, C, McIntosh, J, Della Peruta, M, Kymalainen, H, Tuddenham, EG, Buckley, SM *et al.* (2012). AAV-mediated gene transfer in the perinatal period results in expression of FVII at levels that protect against fatal spontaneous hemorrhage. *Blood* **119**: 957–966.
 43. Wu, Z, Sun, J, Zhang, T, Yin, C, Yin, F, Van Dyke, T *et al.* (2008). Optimization of self-complementary AAV vectors for liver-directed expression results in sustained correction of hemophilia B at low vector dose. *Mol Ther* **16**: 280–289.
 44. Zhou, M, Wang, T, Fu, J, Xiao, G and Liu, Y (2015). Nonoptimal codon usage influences protein structure in intrinsically disordered regions. *Mol Microbiol* **97**: 974–987.
 45. Powell, SK, Rivera-Soto, R and Gray, SJ (2015). Viral expression cassette elements to enhance transgene target specificity and expression in gene therapy. *Discov Med* **19**: 49–57.
 46. Bullock, TN and Eisenlohr, LC (1996). Ribosomal scanning past the primary initiation codon as a mechanism for expression of CTL epitopes encoded in alternative reading frames. *J Exp Med* **184**: 1319–1329.
 47. Mingozzi, F, Maus, MV, Hui, DJ, Sabatino, DE, Murphy, SL, Rasko, JE *et al.* (2007). CD8(+) T-cell responses to adeno-associated virus capsid in humans. *Nat Med* **13**: 419–422.
 48. Mingozzi, F and High, KA (2013). Immune responses to AAV vectors: overcoming barriers to successful gene therapy. *Blood* **122**: 23–36.
 49. Lisowski, L, Dane, AP, Chu, K, Zhang, Y, Cunningham, SC, Wilson, EM *et al.* (2014). Selection and evaluation of clinically relevant AAV variants in a xenograft liver model. *Nature* **506**: 382–386.
 50. Vercauteren, K, Hoffman, BE, Zolotukhin, I, Keeler, GD, Xiao, JW, Basner-Tschakarjan, E *et al.* (2016). Superior *In vivo* Transduction of Human Hepatocytes Using Engineered AAV3 Capsid. *Mol Ther* **24**: 1042–1049.
 51. Zinn, E, Pacouret, S, Khaychuk, V, Turunen, HT, Carvalho, LS, Andres-Mateos, E *et al.* (2015). *In silico* reconstruction of the viral evolutionary lineage yields a potent gene therapy vector. *Cell Rep* **12**: 1056–1068.
 52. Ehrhardt, A, Xu, H and Kay, MA (2003). Episomal persistence of recombinant adenoviral vector genomes during the cell cycle *in vivo*. *J Virol* **77**: 7689–7695.
 53. Wang, L, Wang, H, Bell, P, McMenamin, D and Wilson, JM (2012). Hepatic gene transfer in neonatal mice by adeno-associated virus serotype 8 vector. *Hum Gene Ther* **23**: 533–539.
 54. Coppoletta, JM and Wolbach, SB (1933). Body length and organ weights of infants and children: a study of the body length and normal weights of the more important vital organs of the body between birth and twelve years of age. *Am J Pathol* **9**: 55–70.
 55. Nathwani, AC, Gray, JT, McIntosh, J, Ng, CY, Zhou, J, Spence, Y *et al.* (2007). Safe and efficient transduction of the liver after peripheral vein infusion of self-complementary AAV vector results in stable therapeutic expression of human FIX in nonhuman primates. *Blood* **109**: 1414–1421.
 56. Meliani, A, Boisgerault, F, Ronzitti, G, Collaud, F, Leborgne, C, Kishimoto, TK and Mingozzi, F. (2016) Antigen-specific modulation of capsid immunogenicity with tolerogenic nanoparticles results in successful AAV vector readministration. *Mol Ther* **24**: S34.
 57. Li, H, Haurigot, V, Doyon, Y, Li, T, Wong, SY, Bhagwat, AS *et al.* (2011). *In vivo* genome editing restores haemostasis in a mouse model of haemophilia. *Nature* **475**: 217–221.
 58. Anguela, XM, Sharma, R, Doyon, Y, Miller, JC, Li, H, Haurigot, V *et al.* (2013). Robust ZFN-mediated genome editing in adult hemophilic mice. *Blood* **122**: 3283–3287.
 59. Barzel, A, Paulk, NK, Shi, Y, Huang, Y, Chu, K, Zhang, F *et al.* (2015). Promoterless gene targeting without nucleases ameliorates hemophilia B in mice. *Nature* **517**: 360–364.
 60. Thummel, C, Tjian, R and Grodzicker, T (1982). Construction of adenovirus expression vectors by site-directed *in vivo* recombination. *J Mol Appl Genet* **1**: 435–446.
 61. Ayuso, E, Mingozzi, F, Montane, J, Leon, X, Anguela, XM, Haurigot, V *et al.* (2010). High AAV vector purity results in serotype- and tissue-independent enhancement of transduction efficiency. *Gene Ther* **17**: 503–510.
 62. Matsushita, T, Elliger, S, Elliger, C, Podsakoff, G, Villarreal, L, Kurtzman, GJ *et al.* (1998). Adeno-associated virus vectors can be efficiently produced without helper virus. *Gene Ther* **5**: 938–945.
 63. Ying, BW, Fourmy, D and Yoshizawa, S (2007). Substitution of the use of radioactivity by fluorescence for biochemical studies of RNA. *RNA* **13**: 2042–2050.
 64. Cornelius, CE and Arias, IM (1972). Animal model of human disease. Crigler-Najjar Syndrome. Animal model: hereditary nonhemolytic unconjugated hyperbilirubinemia in Gunn rats. *Am J Pathol* **69**: 369–372.
 65. Montenegro-Miranda, PS, Pañeda, A, ten Bloemendaal, L, Duijst, S, de Waart, DR, Gonzalez-Aseguinolaza, G *et al.* (2013). Adeno-associated viral vector serotype 5 poorly transduces liver in rat models. *PLoS One* **8**: e82597.



This work is licensed under a Creative Commons Attribution-NonCommercial-NoDerivs 4.0 International License. The images or other third party material in this article are included in the article's Creative Commons license, unless indicated otherwise in the credit line; if the material is not included under the Creative Commons license, users will need to obtain permission from the license holder to reproduce the material. To view a copy of this license, visit <http://creativecommons.org/licenses/by-nc-nd/4.0/>

© G Ronzitti *et al.* (2016)

Supplementary Information accompanies this paper on the *Molecular Therapy—Methods & Clinical Development* website (<http://www.nature.com/mtm>)